

## Electric-field effects on the diffusion of Si and Ge adatoms on Si(001) studied by density functional simulations

Yao He<sup>1</sup> and J. G. Che<sup>2</sup><sup>1</sup>*Department of Physics, Yunnan University, Kunming 650091, China*<sup>2</sup>*Department of Physics, Fudan University, Shanghai 200433, China*

(Received 4 March 2009; published 24 June 2009)

We present results of density functional theory (DFT) calculations of the electric-field effects on the clean Si(001) surface and the diffusion of Si or Ge adatoms on Si(001) surface. Our results indicate that the electric field only slightly affected the dimer bond lengths and buckling angles of the clean Si(001), implying that the electric field of scanning tunneling microscopy tip should not be responsible for the observation of symmetric dimers and the flip-flop motion of the buckling dimers. Also, the electric field mainly influences the diffusion along the dimer row, and the diffusion barrier could be reduced greatly under a positive electric field. It can be expected that the positive field should make the diffusion of Si or Ge adatoms on the Si(001) surface become more anisotropic.

DOI: [10.1103/PhysRevB.79.235430](https://doi.org/10.1103/PhysRevB.79.235430)

PACS number(s): 68.35.Fx, 68.37.Ef, 68.43.Bc, 68.43.Jk

### I. INTRODUCTION

The diffusion of single atom on surface is a fundamental process determining the surface morphology developing in epitaxial growth. The rate at which atoms migrate across the surface in comparison to the rate at which they become incorporated at steps, nucleate into new islands, or become absorbed into the bulk strongly influences the nature of the growth process. This close connection between atom transport and crystal growth suggests that it may be possible to modify the properties of solid materials by altering the rate and/or the mechanism of atom diffusion on surfaces. However, in order to carry out this type of “materials engineering” it is necessary not only to understand the details of how atoms and clusters move on surfaces, but also to find ways to control their dynamic behavior on surface.

In past investigations of adatom migration with the field ion microscope (FIM) and scanning tunneling microscopy (STM), it has been shown that an external electric field can affect diffusion behavior of atoms and dimers on surface.<sup>1–6</sup> Kellogg<sup>1</sup> found that the electric field can change the diffusion mechanism from exchange to hopping for self-diffusion on Pt(001) when the applied electric field reaches a critical value of 1.5 V/Å. Au adatoms on Au(001) surface can be stabilized by the presence of the tip and energy barriers for diffusion processes under the STM tip are reduced.<sup>2</sup> Sagisaka *et al.*<sup>6</sup> think that it is possible to manipulate the Si(001) surface phases between  $c(4 \times 2)$  and  $p(2 \times 2)$  by precise sample bias control in STM. According to recent first-principles calculations implementing under an external electric field, there has been strong evidence that diffusion of adsorbates can be significantly influenced by an external electric field.<sup>5,7,8</sup> The stable adsorption site of Ag on Si(111) will be changed from fcc site to top site as applied electric field reaches a value of 1.2 V/Å. The surface diffusion rate of Ag on Si(111) will enhance gradually with increasing field strength, and rapidly reach a maximum value as field being 1.2 V/Å.<sup>7</sup>

We further investigate the electric-field effects on the dynamic behavior of Si (Ge) adatoms on Si(001) surface, since control of fundamental atomistic processes that govern the

surface kinetics of epitaxial growth of Si-Ge materials is of considerable scientific interest and technological importance. Although Si(111) is the most popular semiconductor surface in academic research, Si(001) is a dominant substrate for electronic devices in silicon industry. Compared to complex reconstructions of Si(111), Si(001) is the simplest and the technologically relevant surface of silicon. The common feature of Si(001) surface is the main building block—surface dimer. The surface atoms on Si(001) have two dangling bonds each and will rebond pairwise to form symmetric or buckling dimers in order to reduce the number of dangling bonds. The dimerization is a key factor to determine the surface properties, especially the surface dynamics at Si(001). Previous STM observations have suggested that the diffusion of Si (Ge) adatoms on Si(001) surface is very anisotropic: the surface migration of Si (Ge) adatoms is at least 1000 times faster along the dimer row than perpendicular to them, and the diffusion barrier in the fast direction is estimated to be 0.67 (0.62) eV.<sup>9,10</sup> The *ab initio* calculations<sup>11–17</sup> have confirmed the experimental results. These *ab initio* studies unambiguously determined the location of the binding site and the saddle point of the Si (Ge) adatoms on Si(001) surface (see Fig. 1) as well as the precise configuration of the surface dimers in the vicinity of the adatoms. Therefore, our investigation is concentrated on the electric-field effects on the diffusion barrier of Si (Ge) adatoms on Si(001) surface. Our *ab initio* calculations will present valuable information about dynamic behavior of Si (Ge) on Si(001) and will further confirm our conclusions about surface diffusion under an external electric field, which were obtained from our calculations based on an assumption of the surface with a simple  $(1 \times 1)$  structure.<sup>7</sup> Thus, this technique allows us to control surface dynamic process by turning on and off an external electric field.

### II. METHODS

Our calculations were set up as follows: the initial atomic configuration for our calculations is taken to be the well-known minimum-energy  $c(4 \times 2)$  reconstruction. Our calcu-

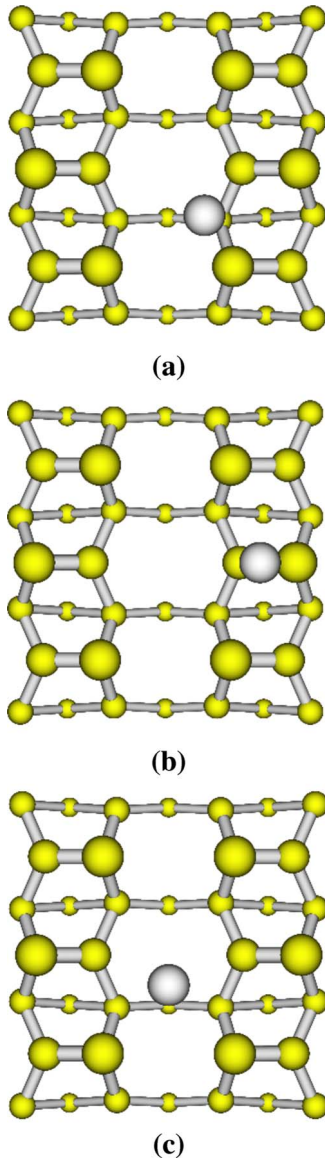


FIG. 1. (Color online) Geometries of the binding site (a), the saddle point along the dimer row (b) and the saddle point across the dimer row (c) for Si or Ge adatoms diffusing on Si(001) surface. Only the three topmost atomic layers are shown. The size of each circle reflects the atom's proximity to the observer.

lations are performed using a slab with ten atomic layers, separated by 20 Å of vacuum. A  $4 \times 4$  unit cell is adopted to avoid interaction between adatoms. By varying the thickness of the slab and the width of the vacuum separating the periodic images perpendicular to the surface, it was verified that the selected system size provides energies with an accuracy of the order of 0.03 eV. Single adatoms were placed on each side of the slab. We used VASP code,<sup>18,19</sup> ultrasoft pseudopotentials for interaction between ions and electrons, and local-density approximation for the exchange-correlation functional. The energy cutoff for the plane-wave basis set was set to 150 eV and a  $(2 \times 2 \times 1)$  mesh of  $\mathbf{k}$  points was used for the  $(4 \times 4)$  unit cell. The unit cell used in our calculations contains thus 160 Si atoms and two adatoms (one on each side of the slab). To include the effect of an external electric

field, the external uniform charge sheets are placed in the vacuum on either side of the slab.<sup>20,21</sup> Throughout our calculations, the direction of the applied external electric field is perpendicular to Si(001) surface, and the positive electric field means that the surface is positively biased.

### III. RESULTS AND DISCUSSIONS

#### A. Clean Si(001)

For clean Si(001), surface atoms of the  $\{001\}$ -truncated silicon crystal have two broken bonds each (i.e., dangling bonds). It is favorable in energy when the surface atoms dimerize to reduce the number of surface dangling bonds. The surface energy can be further lowered by rehybridization, which leads to alternate buckling of the dimers, giving rise to  $c(4 \times 2)$  and  $p(2 \times 2)$  reconstructions. Although asymmetric dimers are expected, it was also argued that the dimers appear to be symmetric in STM images.<sup>22–24</sup> Since STM tip is very close to sample surface, the surface can be subjected to very strong electric field when imaging with an STM, which has been invoked to explain the observation of apparently symmetric dimers.<sup>25,26</sup> Even it is suggested that the  $c(4 \times 2)$  surface can be changed into the  $p(2 \times 2)$  through a flip-flop motion of the buckling dimers by using a sample bias voltage control.<sup>6</sup>

In order to reveal whether the electric field of STM tip should be responsible for the observation of symmetric dimers and the flip-flop motion of the buckling dimers, we have carried out first-principles calculations on the clean Si(001) surface. It is found that the surface energy of asymmetric  $c(4 \times 2)$  reconstruction is indeed lower than that of symmetric  $(2 \times 1)$  reconstruction, and the energy difference is 0.20 eV/dimer. For asymmetric  $c(4 \times 2)$  reconstruction, a dimer bond length of 2.36 Å and a buckling angle of 18.5° are obtained. For symmetric  $(2 \times 1)$  reconstruction, we find a dimer bond length of 2.31 Å. All of these results are in excellent agreement with the other investigations.<sup>27</sup> Then, we applied the electric field on Si(001)  $c(4 \times 2)$  surface. The results show that the dimer bond length and buckling angle are only slightly affected by the electric field. Under an electric field of 0.5 V/Å, which is comparable with the ordinarily tip-induced field in STM, the dimer bond length is 2.36 Å and the buckling angle is 18.0°. Even under a strong field of 2.0 V/Å, the dimer bond length is 2.36 Å and the buckling angle is 16.0°. We have not found that an asymmetric dimer will change to a symmetric one or the flip-flop motion of the buckling dimers will arise, implying that the electric field of STM tip should not be responsible for the observation of the symmetric dimers and the flip-flop dimers. Interestingly, the dimer bond length is almost kept constant and the buckling angle is somewhat reduced under the electric field.

#### B. Si on Si(001)

We begin by studying the binding site of a Si adatom on Si(001). Similar to previous *ab initio* calculations,<sup>11–13</sup> our calculations confirm the most stable binding site suggested by Brocks *et al.*,<sup>11</sup> refer to Fig. 1(a), on which the adatom is

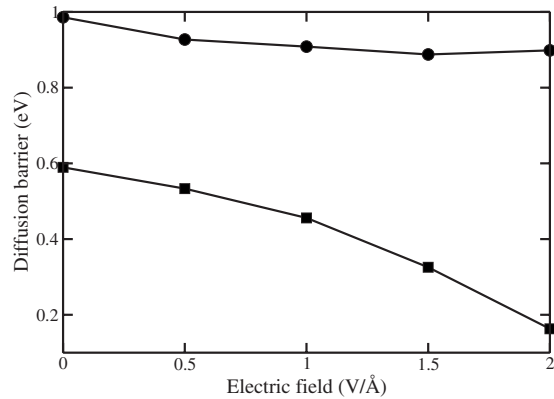


FIG. 2. Field dependence of the diffusion barriers for a Si adatom diffusing on Si(001) surface along two directions. Squares represent the direction along the dimer row, and filled circles represent the direction across the dimer row.

bonded to two dimers of the same row and sits in the trough between the rows. This can be expected since the adatom localized at the binding site rehybrids with the atoms of two dimers of the same dimer row (the bond lengths to up and down Si atoms are 2.37 and 2.36 Å, and the bond angles are 68.3° and 67.0°, respectively). The adatom forms thus only a weak bond with subsurface atoms.

Then we consider the diffusion of Si adatoms on Si(001). On Si(001) surface, the presence of dangling bonds, the directionality of bonding, and surface reconstruction produce multiple adsorption sites as well as complex diffusion pathways. It has been well-established by Brocks *et al.*<sup>11</sup> that there are two diffusion directions for Si adatoms on Si(001), that is, the fast-diffusion direction along the dimer row and the slow-diffusion direction across the dimer row. The saddle point along the dimer row is almost located on the top of a dimer, and the saddle point across the dimer row is located near the center of two dimers cross the trough between the rows [refer to Figs. 1(b) and 1(c)]. Exhaustive searching for diffusion paths is CPU time consuming, since one should locate the maximum energy along each possible path in the complete configuration space, which connects the configurations of the two binding sites. We will thus adopt the suggestions of Brocks *et al.*,<sup>11</sup> namely, there are two possible diffusion paths along and across the dimer rows. The diffusion of Si adatom takes place on top of dimers and not in the interdimer channel. According to our calculations, the diffusion barriers along and across the dimer row are 0.59 and 1.00 eV, respectively. When sitting at the saddle point along the dimer row, the bond lengths of Si adatom to the up and down atoms are 2.32 and 2.32 Å, and the bond angles are 33.4° and 30.2°, in good agreement with previous *ab initio* calculations.<sup>11–13,17</sup>

In order to investigate how electric field influences surface diffusion, we apply then an electric field to the surface and calculate the diffusion barriers along and across the dimer row as a function of electric-field strength. The results are illustrated in Fig. 2, which shows that the diffusion barrier decreases monotonically with increase in the field strength. The diffusion barrier along the dimer row decreases more rapidly than that across the dimer row. When the ap-

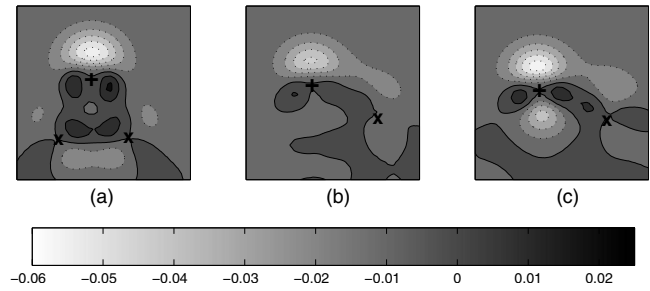


FIG. 3. Charge-density difference ( $e/\text{Å}^3$ ) plots for the saddle point along the dimer row (a), binding site (b) and the saddle point across the dimer row (c) of Si adatom diffusing on Si(001) surface at an electric field of 2.0 V/Å.

plied electric field reaches 2.0 V/Å, the diffusion barrier along the dimer row decreases 0.43 eV, from 0.59 to 0.16 eV, and the diffusion barrier across the dimer row only decreases about 0.1 eV in the range of the field strength we have applied (see Fig. 2). The electric field mainly affects the diffusion along the dimer row, meaning that the diffusion of Si adatom on Si(001) surface will become more anisotropic under an external electric field. In addition, we have studied the electric-field effects on the energetics and diffusion for Si adatom on Si(001) with the symmetric dimers. The results are essentially similar to that with the buckling dimers above.

We now turn to the question why the electric field has different effects on different diffusion directions. From Fig. 2, the changes in the diffusion barriers show that the electric-field effects introduce quadratic or higher terms. This suggests that it may be a consequence of the interaction between surface dipole and the applied electric field. Thus, we calculated the surface dipoles for the binding site and saddle points at different field by a direct integration of the charge densities starting from the center of the slab into the middle of the vacuum region.<sup>28</sup> In our case, the applied electric field will induce charge rearrangement to shield the bulk from the external field, and the induced dipole should be positive (point outward). Our calculations indicate that the induced dipole is always positive and the magnitude of the saddle point (along the dimer row) is always larger than that of the binding site. Since the field-induced dipole should always lower the energy of the system, the dipole is going to further favor the saddle point (along the dimer row) over the binding site. At the electric field of  $E=0.5$  V/Å, the difference of surface dipole between the binding site and saddle point (along the dimer row) is 0.11 (electron\* Angstrom), consistent with the energy difference of 0.06 eV. At higher field, the field dependence is more complicated, since the total field is not uniform at the adatom site and there will be some energy modifications due to changes in bonding configurations manifested in the change in exchange-correlation energies as the charge-density distribution is different.

To examine the field effects on charge and bonding of Si adatom, we plot the pseudocharge difference in Fig. 3. It is obtained by subtracting the charge obtained in two separate calculations: one with and the other without an electric field of 2 V/Å. The atomic positions remain the same in both calculations and correspond to the optimally determined un-

der the electric field. Figures 3(a)–3(c) illustrate the pseudo-charge difference under an electric field of  $2 \text{ V}/\text{\AA}$  for the case of Si adatom on the saddle point (along the dimer row), the binding site and the saddle point (across the dimer row) of Si(001) surface, respectively. In Fig. 3 the region encompassed by dashed lines indicates a depletion of electrons, while the region encompassed by solid lines means an excess of electrons. The symbols + and  $\times$  in the figure indicate positions of Si adatom and Si atom bonded to adatom, respectively.

It can be clearly seen that from Fig. 3(a), for Si adatom at the saddle point along the dimer row, charge above the Si adatom is removed to screen the electric field, while charge in the bonding region between adatom and substrate Si is accumulated. Therefore, the strength of this bond is enhanced. However, this effect is less for Si adatom at the binding site [Fig. 3(b)] and saddle point (across the dimer row) [Fig. 3(c)]. It can be understood by considering the fact that when Si adatom is sitting at the saddle point (along the dimer row), the direction of the bond between adatom and substrate Si is about  $30^\circ$  tilted to the field direction, while the tilted angle is about  $65^\circ$  for Si adatom at the binding site (for both cases, the Si adatom forms two bonds with substrate Si atoms). Consequently, the bond at saddle point (along the dimer row) experiences stronger field effect than that of the binding site. It is obvious that the polarizability and the field-dipole interaction at the saddle point (along the dimer row) will increase with the field strength, and will be weakened at the binding site. As Figs. 3(b) and 3(c) show, the situation is almost the same for Si adatom at the binding site and the saddle point (across the dimer row), which accounts for the almost constant diffusion barrier (across the dimer row) under different electric field.

### C. Ge on Si(001)

Because of the technological potential of Si-Ge and Si-GeSi heterojunctions, for example, in high-speed heterobipolar transistors and in optoelectronic devices, the growth of germanium on silicon has been intensively studied for several decades. Qualitatively, Si and Ge are quite similar in their structural and electronic properties. The Ge lattice, however, is expanded by 4.2% with respect to the Si lattice and the Ge-Ge bond is weaker than the Si-Si bond, leading to a smaller surface energy. Thus, the system Ge/Si is usually discussed as a classical model for the Stranski-Krastanov growth mode. In general, Ge atoms deposited onto a Si(001) substrate at room temperature form two-dimensional epitaxial islands and follow the sequence of adatom adsorption, adatom diffusion, nucleation of islands, and growth of dimer row islands just as in silicon homoepitaxy. It is well-known<sup>14</sup> that on clean Si(001) Ge adatom diffusion is highly anisotropic and single atoms move along the dimer row about 1000 times faster than across the dimer rows, similar to Si adatom diffusion on Si(001). The activation barrier for the diffusion of Ge on Si(001) also resembles that for Si, but its vibration frequency is an order of magnitude smaller, implying that Ge adatoms diffuse more slowly on Si(001) than Si adatoms.<sup>10</sup>

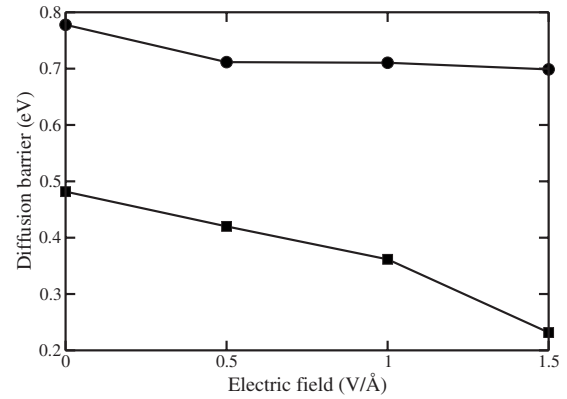


FIG. 4. Field dependence of the diffusion barriers for a Ge adatom diffusing on Si(001) surface along two directions. Squares represent the direction along the dimer row, and filled circles represent the direction across the dimer row.

For Ge adatom on Si(001), our results are similar to that of Si adatom on Si(001). The binding site of Ge on Si(001) is also localized at the same site as the binding site of Si adatom on Si(001), at which the Ge adatom rehybrids with atoms of two dimers in the same dimer row, and the adatom forms only a weak bond with subsurface atoms. Similar to the case of Si adatom on Si(001), the saddle point along the dimer row is located on top of dimer, while the saddle point across dimer row is located near the center of two dimers cross the trough between the rows, refer to Figs. 1(b) and 1(c). The diffusion barriers along and across the dimer row are then calculated being 0.48 and 0.80 eV, respectively, compared to the values of Si adatom (0.59 and 1.0 eV). The calculated bond lengths of Ge adatom to the up and down atoms at binding site are 2.45 and 2.44 Å, and the bond angles are  $66.8^\circ$  and  $65.2^\circ$ . The bond lengths of Ge adatom to the up and down atoms at the saddle point along the dimer row are 2.41 and 2.41 Å, and the bond angles are  $31.7^\circ$  and  $28.5^\circ$ . These results are similar to the case of Si adatoms on Si(001).

Sequentially, we apply an electric field to the surface and calculate the diffusion barriers in two directions as a function of electric-field strength. The results are shown in Fig. 4. The diffusion barrier decreases monotonically with increase in the field strength. The diffusion barrier along the dimer row decreases more rapidly. When the field reaches  $2.0 \text{ V}/\text{\AA}$ , the barrier along the dimer row decreases from 0.48 to  $-0.09 \text{ eV}$ , and the barrier across the dimer row varies less than 0.2 eV throughout all field strength (see Fig. 4). Similar to the case of Si adatoms on Si(001), the electric field mainly influences the diffusion along the dimer row. We could also expect that the diffusion of Ge adatoms on Si(001) surface will become more anisotropic under an external electric field.

We also calculate the surface dipoles for the binding site and saddle point. At  $E=0.5 \text{ V}/\text{\AA}$ , the difference in surface dipole between the binding site and saddle point (intrinsic and induced together) is 0.16 (electron\* Angstrom), which is consistent with the energy difference of 0.08 eV. For Ge adatom diffusing on Si(001) surface, the calculated results are similar to Si adatom on Si(001) surface. As shown in Fig. 5, the charge-density difference for Ge adatom at the saddle

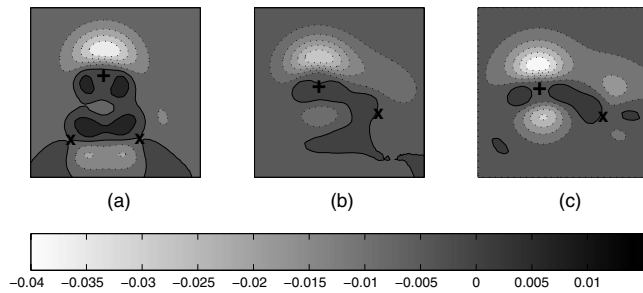


FIG. 5. Charge-density difference ( $e/\text{\AA}^3$ ) plots for the saddle point along the dimer row (a), binding site (b) and the saddle point across the dimer row (c) of Ge adatom diffusing on Si(001) surface at an electric field of  $1.5 \text{ V/\AA}$ .

point and binding site shows similar characters to that of Si adatom (see Fig. 3). Therefore, the electric-field effects on the diffusion of Ge adatom on Si(001) should be analogous to that of Si adatom.

#### IV. CONCLUSIONS

We have carried out first-principles calculations to investigate the electric-field effects on the clean Si(001) surface and the diffusion of Si or Ge adatoms on Si(001) surface. This is a density functional theory (DFT) calculation to study the electric-field effects on such systems, and it provides

strong evidence that the diffusion processes are strongly field dependent. All calculations indicate that the diffusion barrier could be reduced greatly under a positive electric field, and the electric field mainly influences the diffusion barrier along the dimer row. It can be expected that the electric field should make the diffusion of Si or Ge adatoms on Si(001) surface become more anisotropic. However, it is possible that the electric field will lead to lower-energy transition states for diffusion, besides that corresponding to the lowest-energy path without an electric field. The electric-field effects might be even larger for some of the alternative saddle-point geometries that have been found in the work of Huang *et al.*<sup>17</sup> In addition, We have also shown that the electric field only slightly affects the dimer bond length and buckling angle of the clean Si(001). The results imply that the electric field of STM tip should not be responsible for the observation of symmetric dimers and the flip-flop motion of the buckling dimers.

#### ACKNOWLEDGMENTS

This work was supported by the National Natural Science Foundation of China (Grant No. 10804095 and No. 10664006), Applied Basic Research Foundation of Yunnan Province (Grant No. 2008CD062), Science and Technology Promotion Project of Yunnan Province (Grant No. 2007A0017z), as well as Science and Technology Foundation of Yunnan University (Grant No. 2007Z003B).

- <sup>1</sup>G. L. Kellogg, Phys. Rev. Lett. **70**, 1631 (1993).
- <sup>2</sup>M. R. Sørensen, K. W. Jacobsen, and H. Jónsson, Phys. Rev. Lett. **77**, 5067 (1996).
- <sup>3</sup>B. S. Swartzentruber, A. P. Smith, and H. Jónsson, Phys. Rev. Lett. **77**, 2518 (1996).
- <sup>4</sup>J. M. Carpinelli and B. S. Swartzentruber, Phys. Rev. B **58**, R13423 (1998).
- <sup>5</sup>L. M. Sanders, R. Stumpf, T. R. Mattsson, and B. S. Swartzentruber, Phys. Rev. Lett. **91**, 206104 (2003).
- <sup>6</sup>K. Sagisaka, D. Fujita, G. Kido, and N. Koguchi, Surf. Sci. **566-568**, 767 (2004).
- <sup>7</sup>Y. He, X. Y. Wei, C. T. Chan, and J. G. Che, Phys. Rev. B **71**, 045401 (2005).
- <sup>8</sup>T. R. Mattsson, B. S. Swartzentruber, R. Stumpf, and P. J. Feibelman, Surf. Sci. **536**, 121 (2003).
- <sup>9</sup>Y. W. Mo, J. Kleiner, M. B. Webb, and M. G. Lagally, Phys. Rev. Lett. **66**, 1998 (1991).
- <sup>10</sup>M. G. Lagally, Jpn. J. Appl. Phys., Part 1 **32**, 1493 (1993).
- <sup>11</sup>G. Brocks, P. J. Kelly, and R. Car, Phys. Rev. Lett. **66**, 1729 (1991).
- <sup>12</sup>Q. M. Zhang, C. Roland, P. Boguslawski, and J. Bernholc, Phys. Rev. Lett. **75**, 101 (1995).
- <sup>13</sup>A. P. Smith, J. K. Wiggs, H. Jónsson, H. Yan, and L. R. Corrales, J. Chem. Phys. **102**, 1044 (1995).
- <sup>14</sup>V. Milman, D. E. Jesson, S. J. Pennycook, M. C. Payne, M. H. Lee, and I. Stich, Phys. Rev. B **50**, 2663 (1994).
- <sup>15</sup>G. M. Dalpian, A. Fazzio, and A. J. R. da Silva, Phys. Rev. B **63**, 205303 (2001).
- <sup>16</sup>A. van de Walle, M. Asta, and P. W. Voorhees, Phys. Rev. B **67**, 041308 (2003).
- <sup>17</sup>L. Huang, F. Liu, and X. G. Gong, Phys. Rev. B **70**, 155320 (2004).
- <sup>18</sup>G. Kresse and J. Furthmüller, Comput. Mater. Sci. **6**, 15 (1996).
- <sup>19</sup>G. Kresse and J. Furthmüller, Phys. Rev. B **54**, 11169 (1996).
- <sup>20</sup>J. G. Che, Z. Z. Zhu, and C. T. Chan, Phys. Rev. Lett. **82**, 3292 (1999).
- <sup>21</sup>J. G. Che and C. T. Chan, Phys. Rev. B **67**, 125411 (2003).
- <sup>22</sup>R. M. Tromp, R. J. Hamers, and J. E. Demuth, Phys. Rev. Lett. **55**, 1303 (1985).
- <sup>23</sup>R. J. Hamers, P. Avouris, and F. Bozso, J. Vac. Sci. Technol. A **6**, 508 (1988).
- <sup>24</sup>R. J. Hamers, R. M. Tromp, and J. E. Demuth, Phys. Rev. B **34**, 5343 (1986).
- <sup>25</sup>P. Badziag, W. S. Verwoerd, and M. A. Van Hove, Phys. Rev. B **43**, 2058 (1991).
- <sup>26</sup>N. Isshiki, H. Kageshima, K. Kobayashi, and M. Tsukada, Ultramicroscopy **42-44**, 109 (1992).
- <sup>27</sup>A. Ramstad, G. Brocks, and P. J. Kelly, Phys. Rev. B **51**, 14504 (1995).
- <sup>28</sup>T. C. Leung, C. L. Kao, W. S. Su, Y. J. Feng, and C. T. Chan, Phys. Rev. B **68**, 195408 (2003).